Lecture 14. Temperature Lidar (4)
Resonance Fluorescence
Fe and K Doppler Lidars

- More Species in the Upper Atmosphere
  - Metal Species
  - Effective Cross-Section Computation
- More Resonance Fluorescence Doppler Lidars
  - K Doppler Lidar
  - Fe Doppler Lidar
  - More Options for Na Doppler Lidar
- Summary

More Resonance Fluorescence Doppler Lidars on More Species

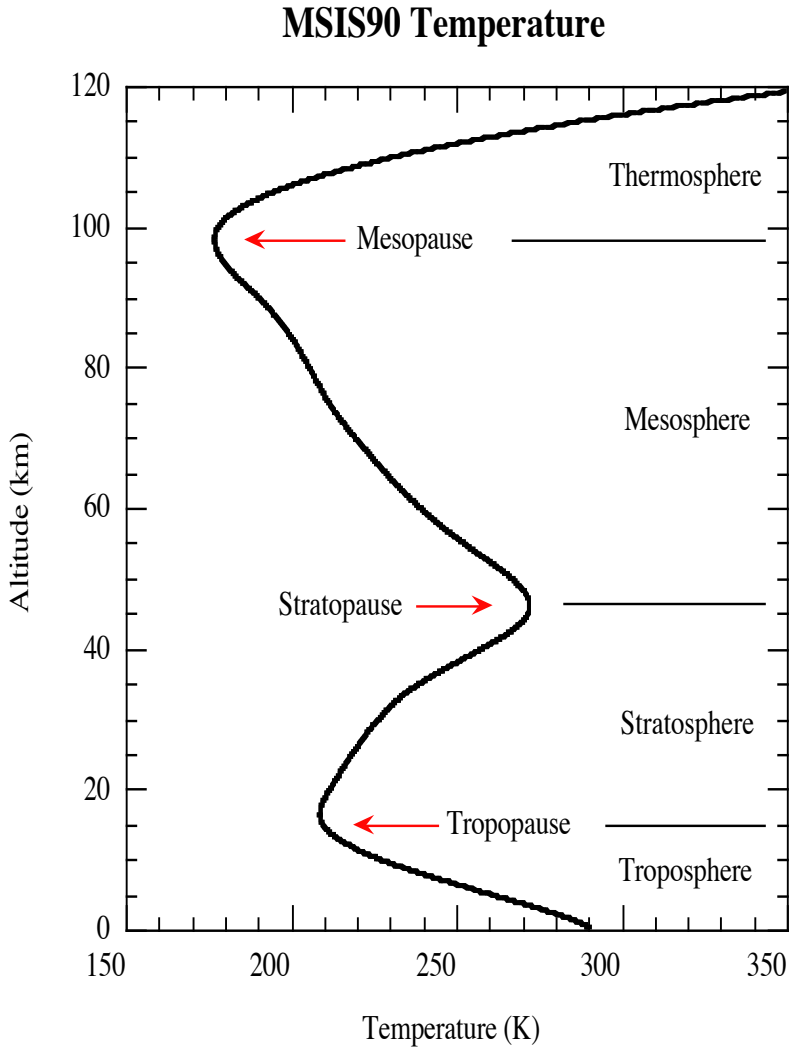

- Besides Na, there are more metal species (K, Fe, Ca, Ca^+, Mg, Li, ...) from meteor ablation and sputtering. They can be used as tracers for Doppler lidar measurements in the MLT region.

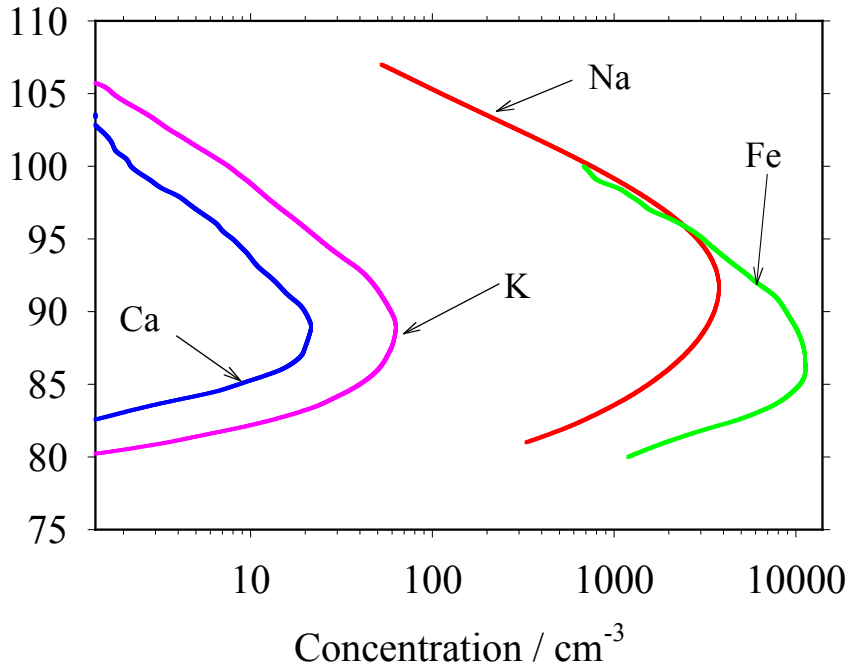

Metal layers are not limited to 110 km, but have been observed to 170 km.

Metal Species in MLT Region

Species	Central wavelength (nm)	A_{ki} ($x10^8$ s^{-1})	Degeneracy g_k / g_i	Atomic Weight	Isotopes	Doppler rms Width (MHz)	σ_0 ($x10^{-12}$ cm^2)	Abundance ($x10^9$ cm^{-2})	Centroid Altitude (km)	Layer rms Width (km)
Na (D_2)	589.1583	0.616	4 / 2	22.98977	23	456.54	14.87	4.0	91.5	4.6
Fe	372.0995	0.163	11 / 9	55.845	54, 56, 57, 58	463.79	0.944	10.2	88.3	4.5
K (D_1)	770.1088	0.382	2 / 2	39.0983	39, 40, 41	267.90	13.42	4.5×10^{-2}	91.0	4.7
K (D_2)	766.702	0.387	4 / 2	39.0983	39, 40, 41	267.90	26.92	4.5×10^{-2}	91.0	4.7
Ca	422.793	2.18	3 / 1	40.078	40, 42, 43, 44, 46, 48	481.96	38.48	3.4×10^{-2}	90.5	3.5
Ca^+	393.777	1.47	4 / 2	40.078	Same as Ca	517.87	13.94	7.2×10^{-2}	95.0	3.6

- In principle, all these species can be used as trace atoms for resonance fluorescence Doppler lidar measurements.
- Whether a Doppler lidar can be developed and used mainly depends on the availability and readiness of laser and electro-optic technologies. In addition, the constituent abundance and absorption cross-section are naturally determined.

Effective Cross Section Computation

- First, the lineshape of absorption cross section for single-frequency laser excitation is the convolution of homogeneous broadening Lorentzian with inhomogeneous Doppler broadening Gaussian, i.e., Voigt lineshape --

$$\sigma_{abs\_s.freq}(\nu) = \sigma_o \cdot g_{abs\_s.freq} = \sigma_o \cdot \left(g_H(\nu) \otimes g_D(\nu)\right)$$

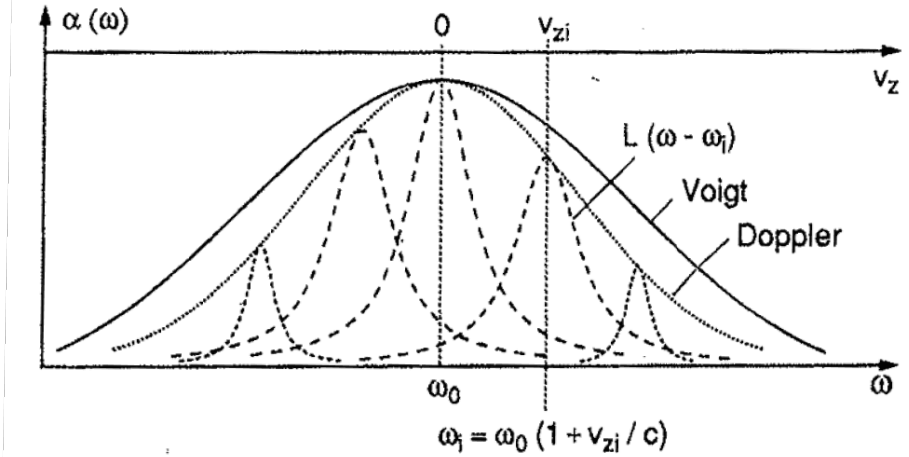

Fig. 3.9. Voigt profile as a convolution of Lorentzian line shapes $L(\omega_0 - \omega_i)$ with $\omega_i = \omega_0(1 + v_{zi}/c)$

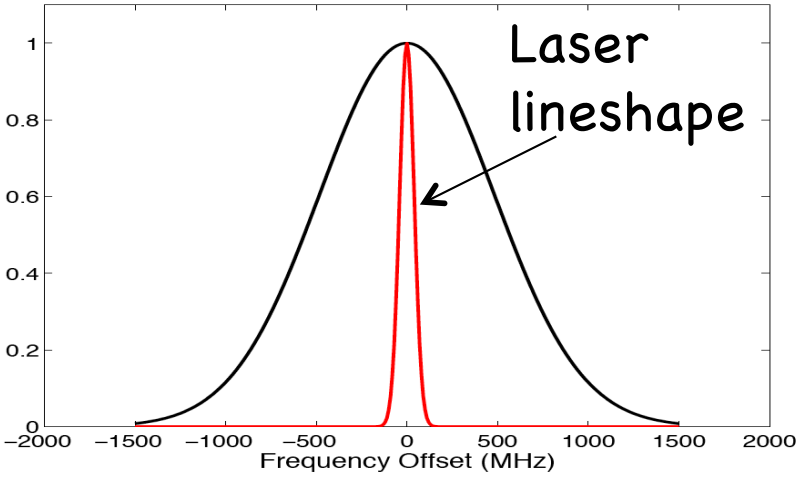

- Second, the lineshape of effective absorption cross section for finite-linewidth laser excitation is the convolution of the above single-freq absorption cross section with the laser lineshape --

$$\sigma_{eff\_abs}(\nu) = \sigma_o \cdot g_{eff\_abs} = \sigma_o \cdot \left(g_{Voigt}(\nu) \otimes g_L(\nu)\right)$$

Effective Cross Section Computation for Species without more-than-one isotopes

- Third, if the species like Na has only one isotope like ^{23}Na but no other isotopes, the lineshape of effective total scattering cross section for finite-linewidth laser excitation is given by the effective absorption cross section multiplied by the branching ratio of resonance fluorescence for the wavelengths that the lidar receiver can receive.

$$\sigma_{eff\_scattering}(\nu) = \sigma_{eff\_abs}(\nu) \cdot R_b$$

- If ignoring the homogeneous broadening like natural linewidth and power broadening, the single-freq absorption cross-section becomes a Gaussian shape. If the laser lineshape is also approximated as a Gaussian, then the overall absorption cross-section is the convolution of two Gaussians, which results in another Gaussian with rms width given by

$$\sigma_e = \sqrt{\sigma_D^2 + \sigma_L^2}$$

Effective Cross Section Computation for Species with more-than-one isotopes

- Third, if the species like K, Fe and Ca have more than one isotopes, σ_{eff_abs} in step 2 is for one isotope. The overall effective absorption cross-section for all isotopes is the weighted sum of all isotopes.

$$\sigma_{eff\_abs}(overall\ \ isotopes) = \sum_{m=1}^{N}\left[\sigma_{eff\_abs,m}(isotope) \times Isotope\ \ Abundance_m\right]$$

- For one isotope, the lineshape of effective total scattering cross-section for finite-linewidth laser excitation is given by the effective absorption cross section multiplied by the branching ratio of resonance fluorescence for the wavelengths that the lidar receiver can receive.

$$\sigma_{eff\_scattering}(\nu) = \sigma_{eff\_abs}(\nu) \cdot R_b$$

- Fourth, the overall all-isotope effective total scattering cross section for finite-linewidth laser excitation is given by the weighted sum of all isotopes. The weight is the isotope abundance in the atmosphere.

$$\sigma_{eff}(overall\ \ isotopes) = \sum_{m=1}^{N}\left[\sigma_{eff,m}(isotope) \times Isotope\ \ Abundance_m\right]$$

Example: Effective Cross-Section for K

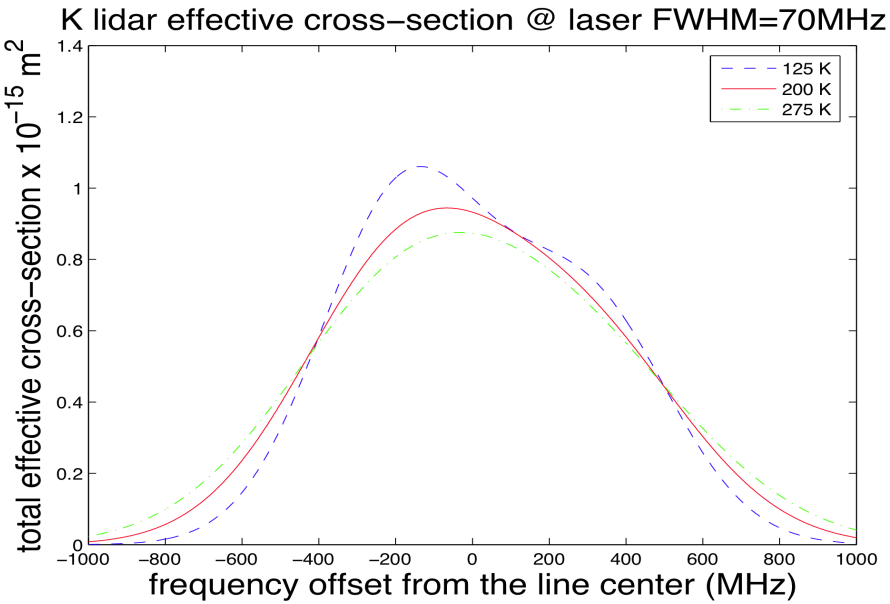

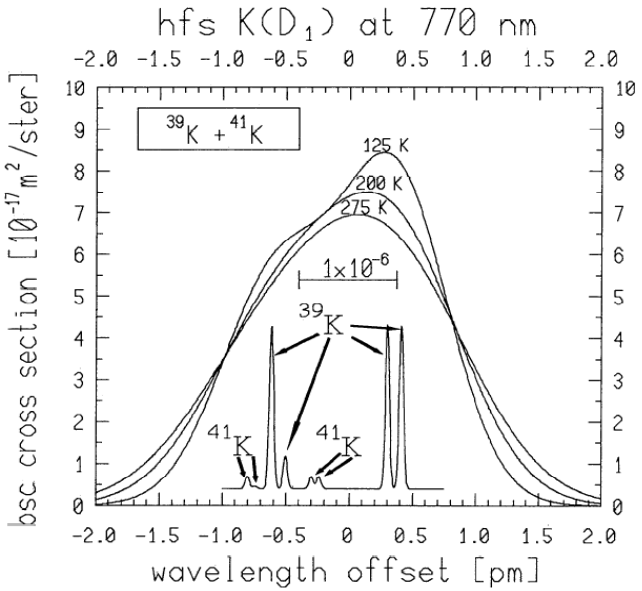

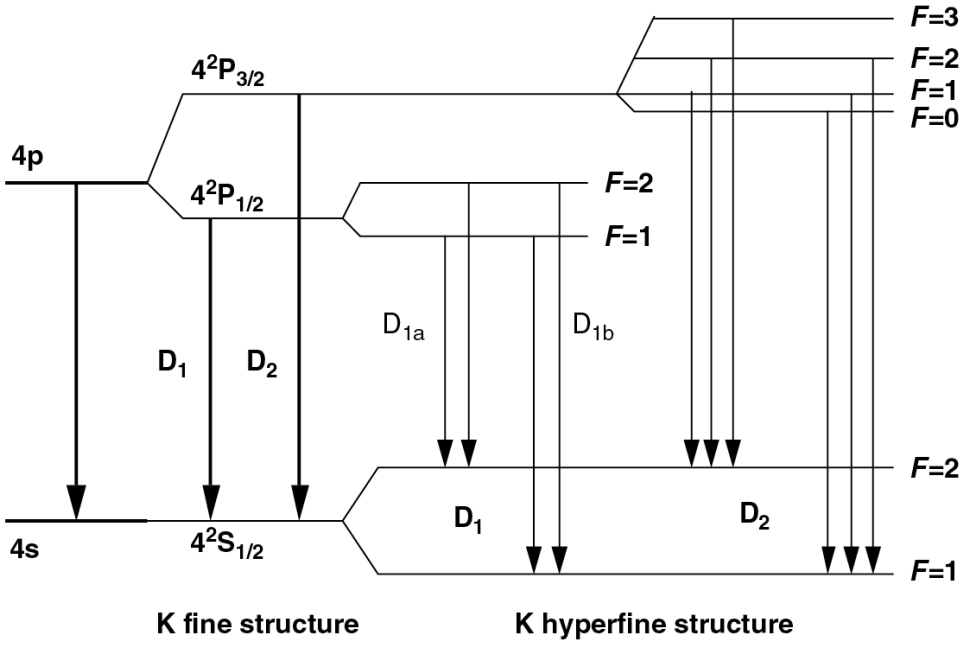

Atomic K energy levels

Reference our textbook Chapter 5

Effective Cross-Section for K Atoms

- Absorption cross section of K atom's D1 line is given by

$$\sigma_{abs}(\nu) = \sum_{A=39}^{41} \left\{ IsotopeAbdn(A) \frac{1}{\sqrt{2\pi}\sigma_D} \frac{e^2 f}{4\varepsilon_0 m_e c} \sum_{n=1}^{4} A_n \exp\left(-\frac{[\nu_n - \nu(1 - V_R/c)]^2}{2\sigma_D^2} \right) \right\} \quad (11.9)$$

Isotope abundance: 93.2581% (^{39}K), 0.0117% (^{40}K), 6.7302% (^{41}K)
Line strength: An = 5/16, 1/16, 5/16, 5/16
Oscillator strength: f, Doppler broadening: σ_D

- The effective total scattering cross section of K atom's D1 line is the convolution of the absorption cross section and the laser lineshape. Under the assumption of Gaussian lineshape of the laser, it is given by

$$\sigma_{eff}(\nu) = \sum_{A=39}^{41} \left\{ IsotopeAbdn(A) \frac{1}{\sqrt{2\pi}\sigma_e} \frac{e^2 f}{4\varepsilon_0 m_e c} \sum_{n=1}^{4} A_n \exp\left(-\frac{[\nu_n - \nu(1 - V_R/c)]^2}{2\sigma_e^2} \right) \right\} \quad (11.10)$$

where $\sigma_e = \sqrt{\sigma_D^2 + \sigma_L^2}$ (11.11) and $\sigma_D = \sqrt{\frac{k_B T}{M\lambda_0^2}}$ (11.12)

Refer to our textbook Chapter 5 and references therein

K Atomic Energy Levels

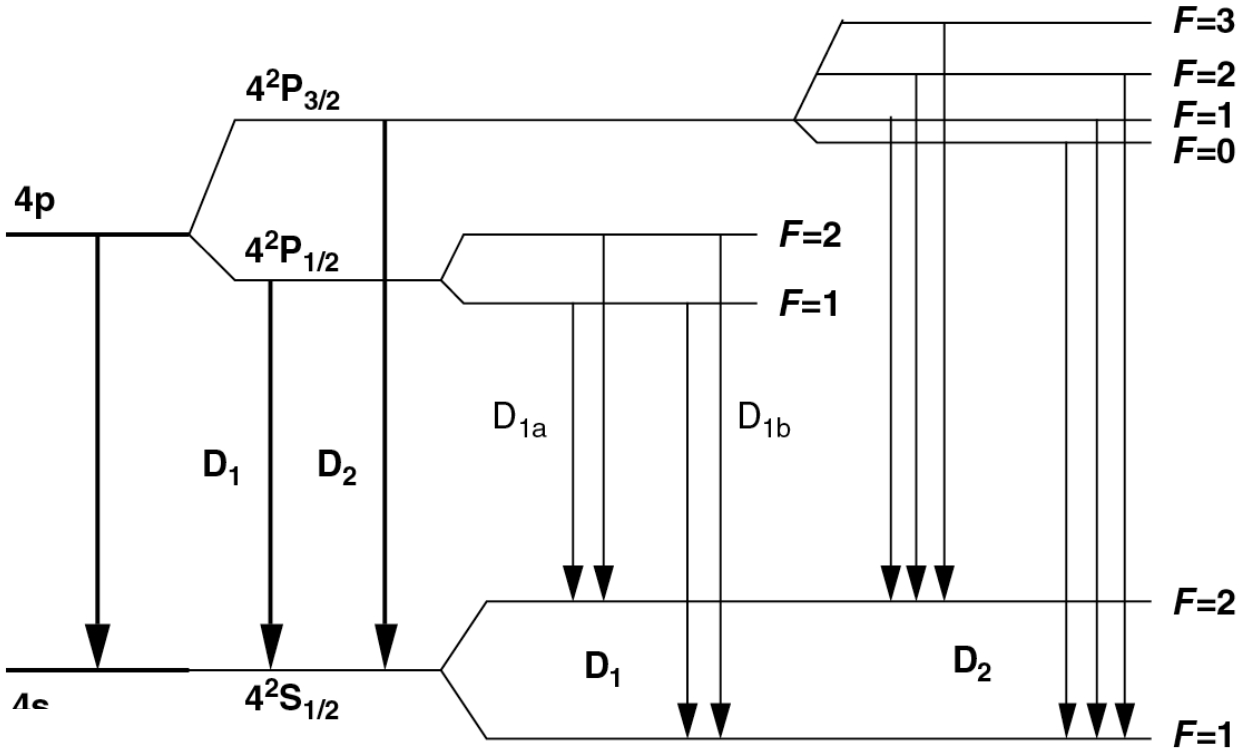

K fine structure K hyperfine structure

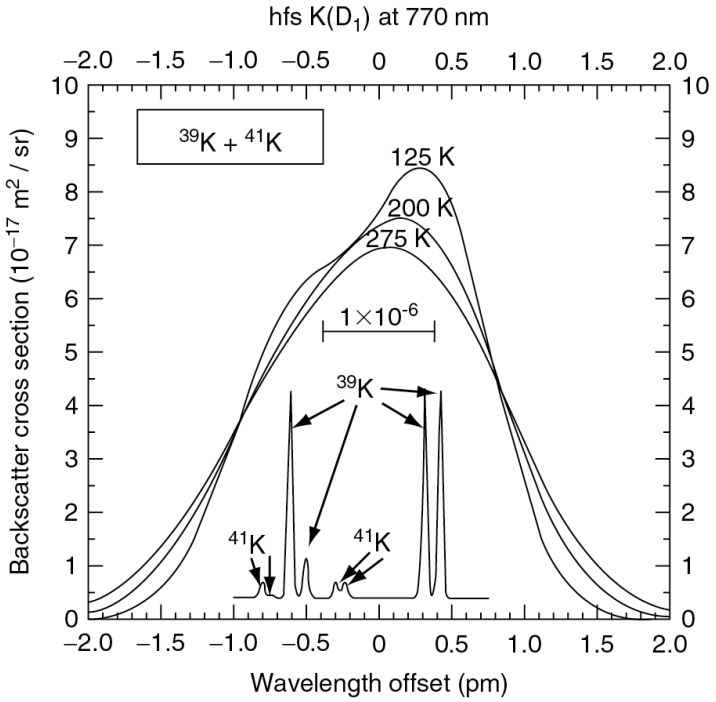

Transition	K(D_1)	K(D_2)
Wavelength air [nm]	769.8974	766.4911
Wavelength vacuum [nm]	770.1093	766.7021
Rel. intensity	24	25
A_{ik} [$10^8 s^{-1}$]	0.382 (±10%)	0.387 (±10%)
f-value	0.340	0.682
Terms $^{2S+1}L_J$	$^2S_{1/2} - ^2P^o_{1/2}$	$^2S_{1/2} - ^2P^o_{3/2}$
$g_i - g_k$	2-2	2-4

K Atomic Parameters

Isotope	Atomic mass	Abundance	Nuclear spin	K(D_1) line shift
39	38.963 706 9(3)	0.932 581(44)	$I = 3/2$	0
40	39.963 998 67(29)	0.000 117(1)	$I = 4$	125.58 MHz
41	40.961 825 97(28)	0.067 302(44)	$I = 3/2$	235.28 MHz

Table 5.8 Quantum Numbers, Frequency Offsets, and Relative Line Strength for K (D_1) Hyperfine Structure Lines

$^2S_{1/2}$	$^2P_{1/2}$	^{39}K (MHz)	^{41}K (MHz)	Relative Line Strength
$F = 1$	$F = 2$	310	405	5/16
	$F = 1$	254	375	1/16
$F = 2$	$F = 2$	−152	151	5/16
	$F = 1$	−208	121	5/16

K Doppler Lidar Principle & Metrics

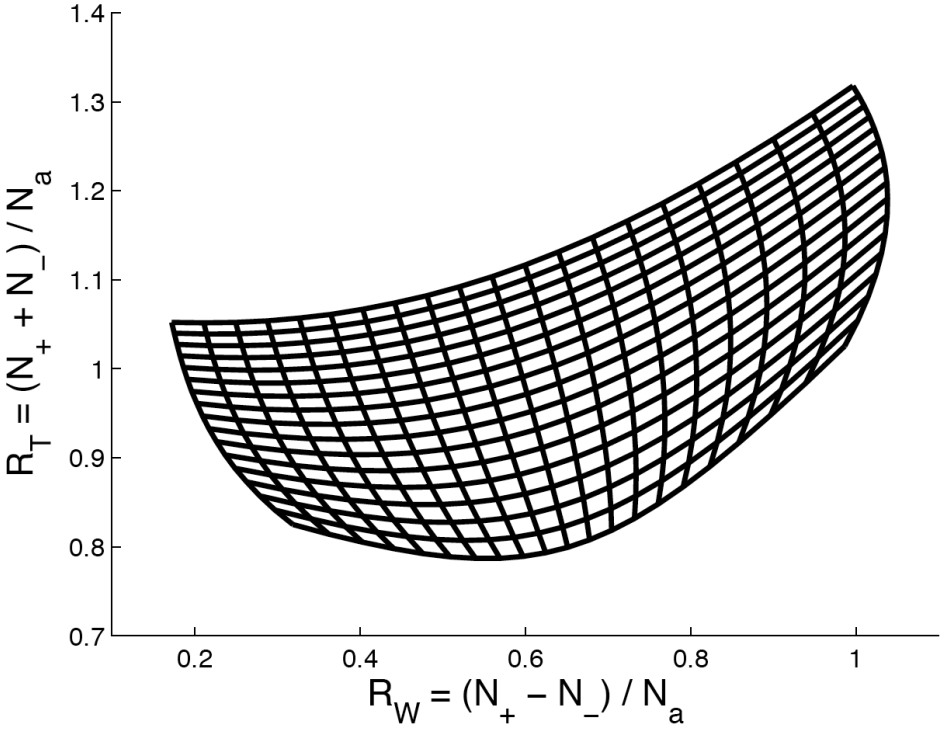

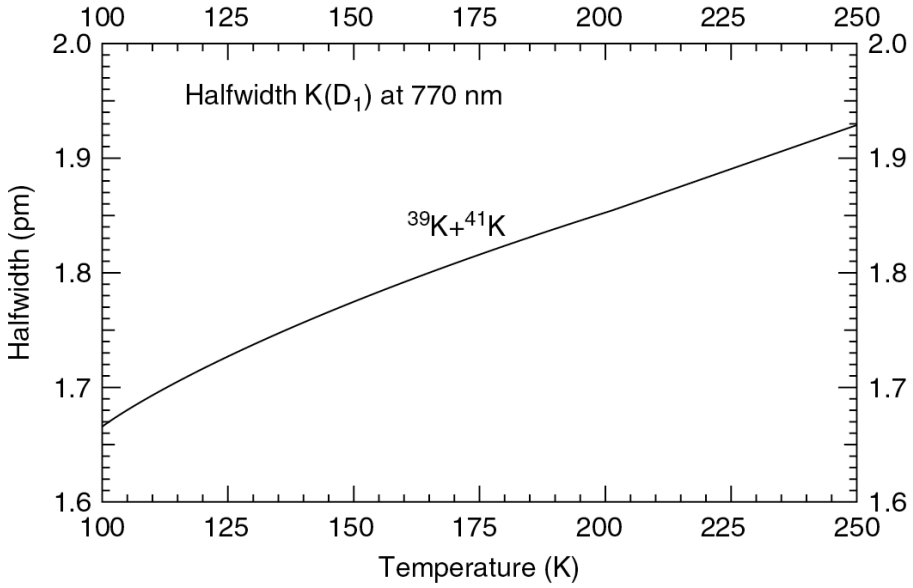

- Ratio technique versus scanning technique
- Scanning technique actually has its advantages on several aspects, depending on the laser system used - whether there is pedestal, background problems, etc.
- Ratio technique usually gives higher resolution.

K Doppler Lidar Instrumentation

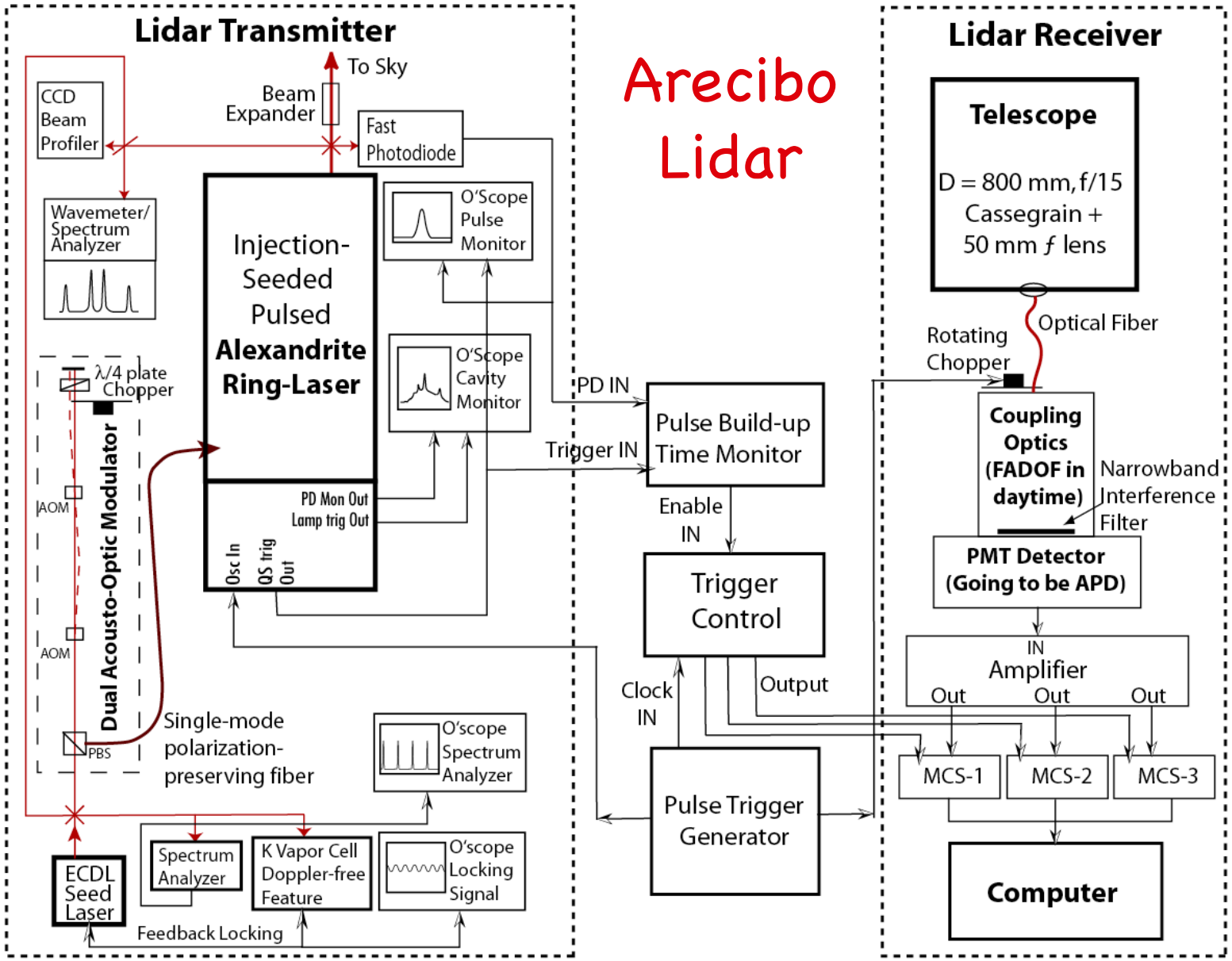

[Friedman and Chu, JGR, 2007]

Arecibo Observatory K Doppler Lidar

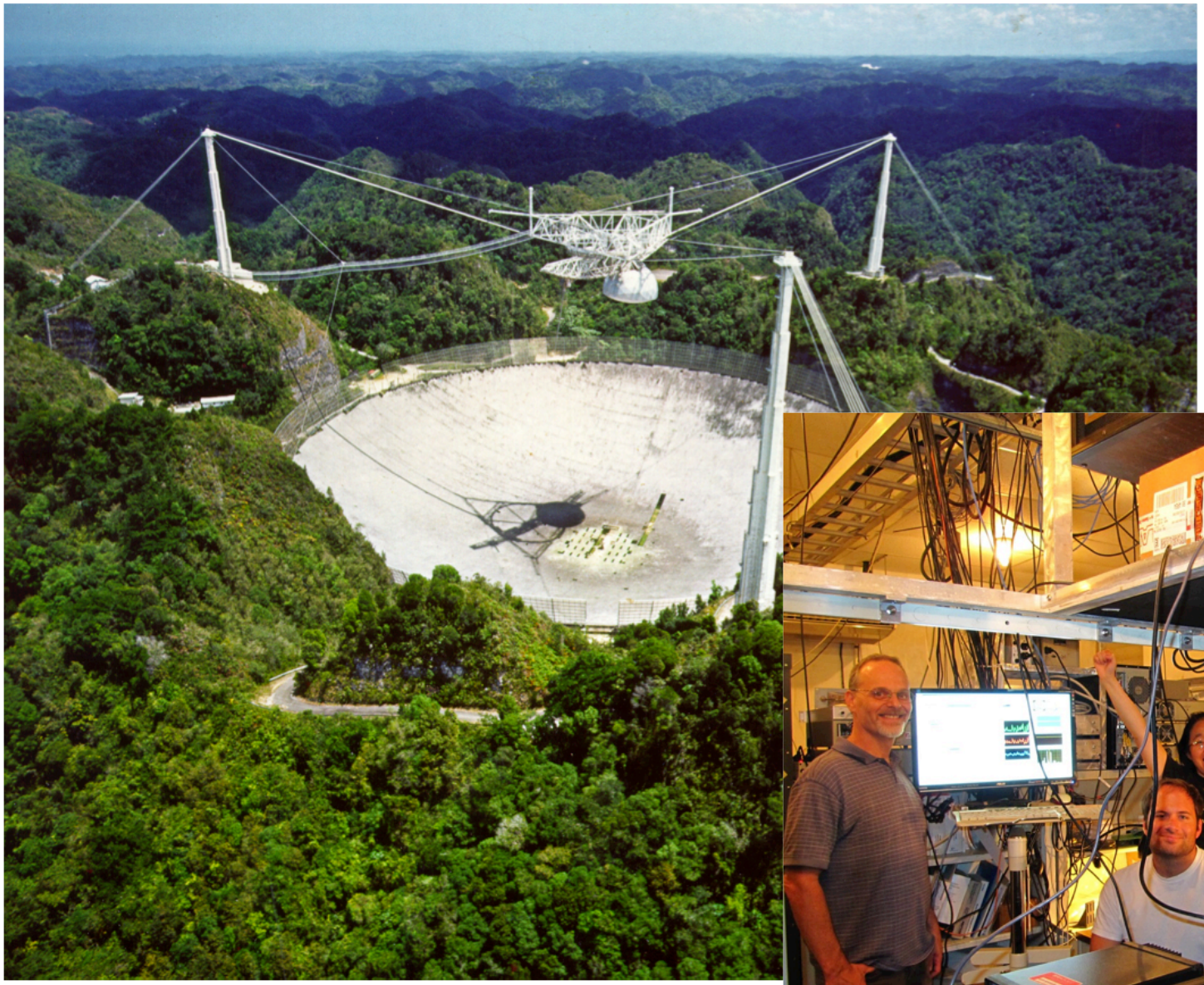

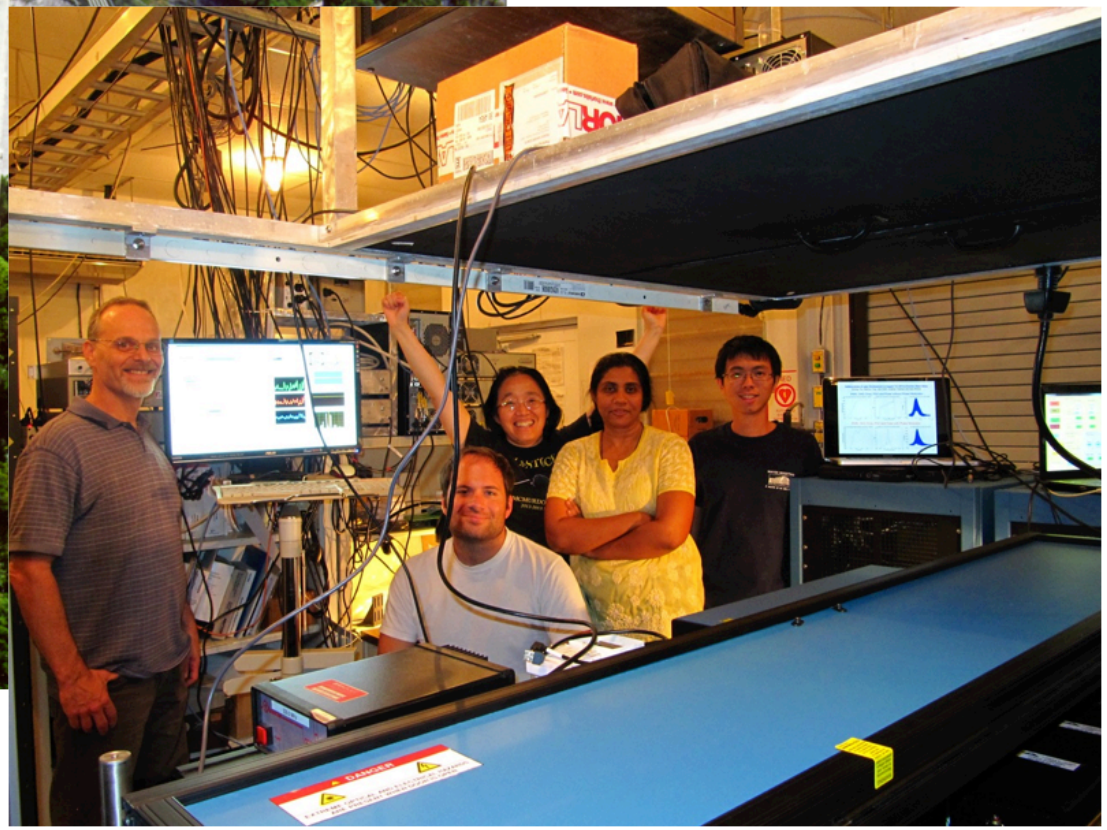

IAP Scanning K Doppler Lidar

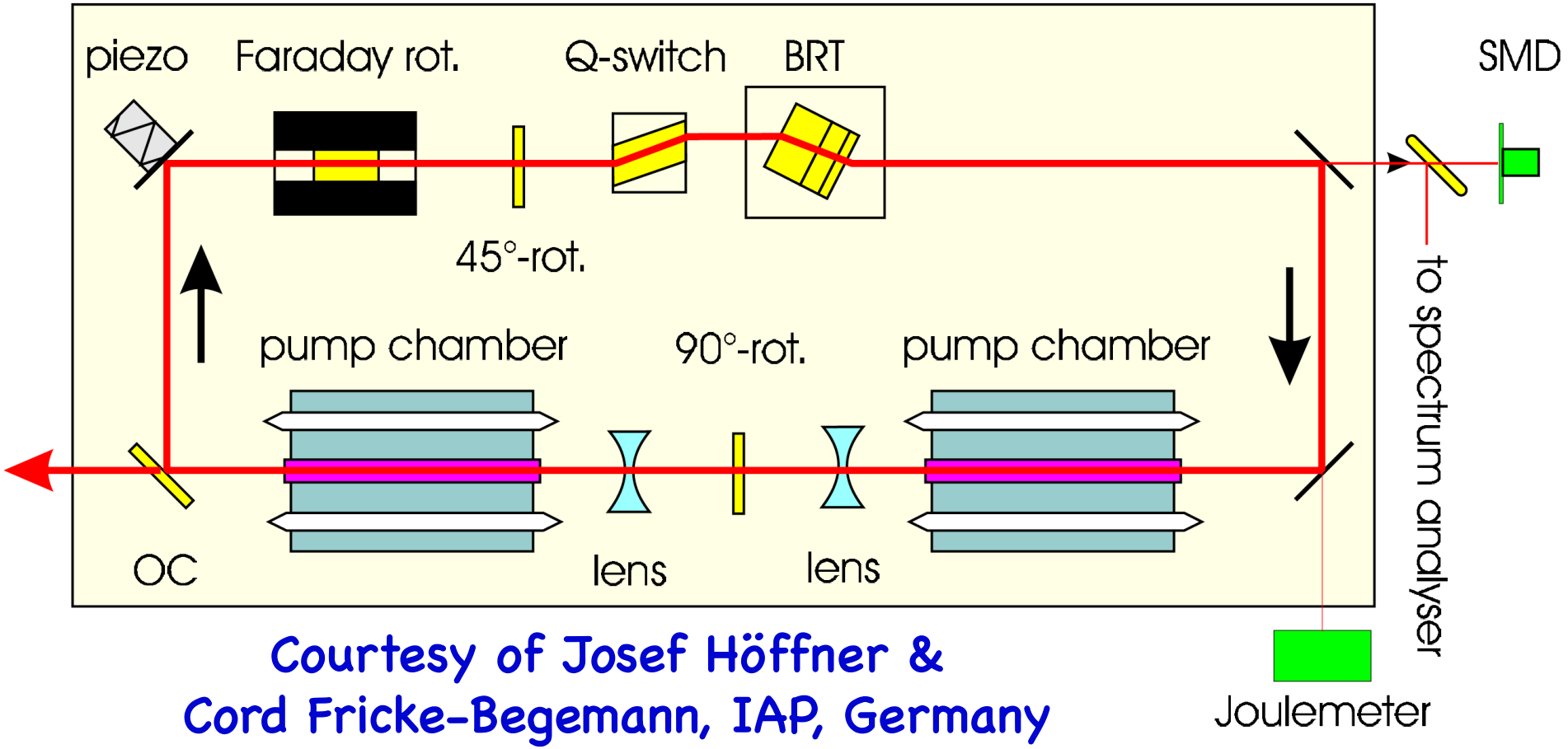

Courtesy of Josef Höffner &
Cord Fricke-Begemann, IAP, Germany

- Based on Light Age, Inc. pulsed alexandrite ring laser, but IAP engineers performed significant in-house development and upgrade.
- The laser frequency is scanned in about 18 channels for temperature-only measurements in MLT region.

Fe Layers from Antarctica Reaching 170 km

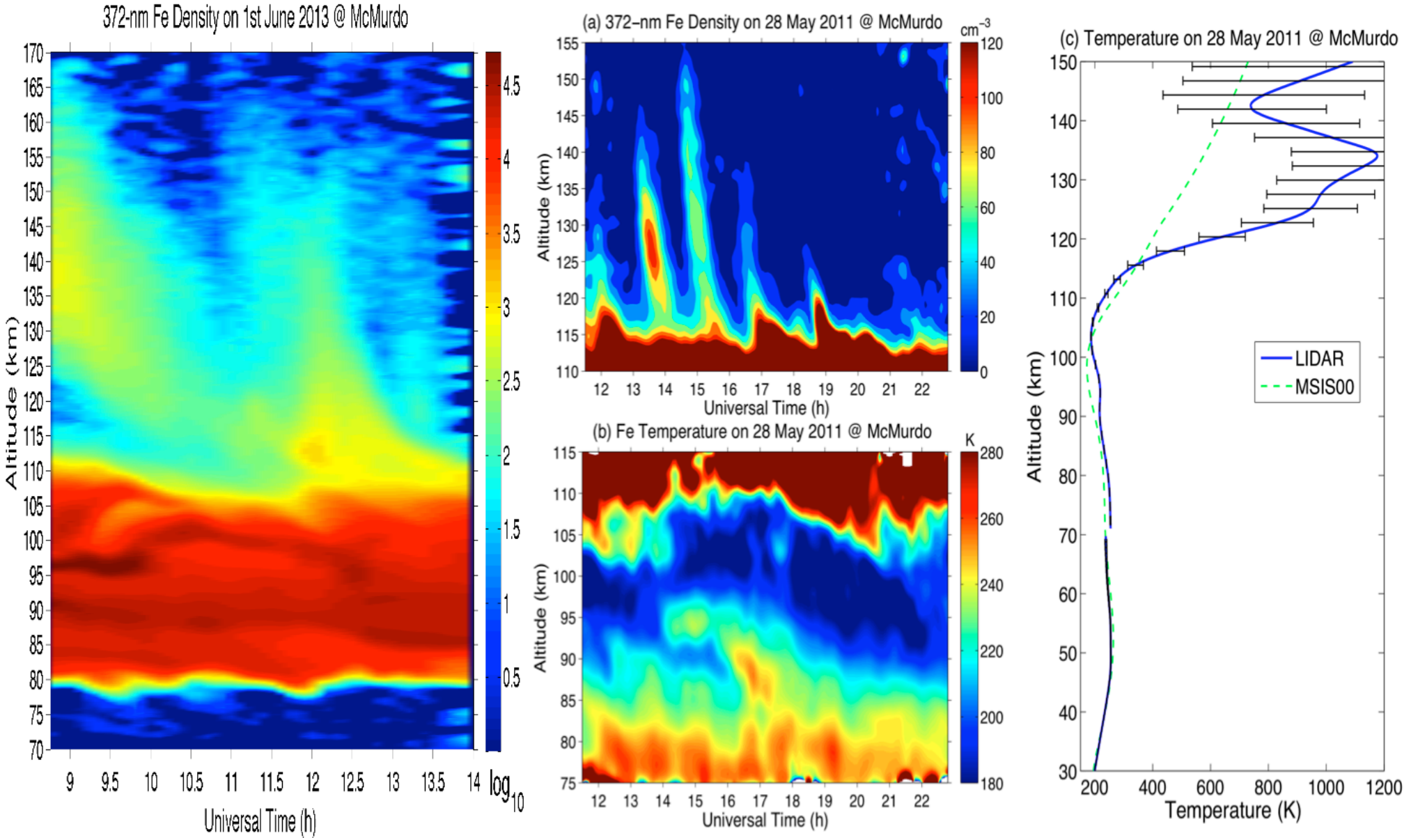

Taken from [Chu et al., CEDAR, 2013] and [Chu et al., GRL, 2011]

Fe Doppler Lidar Principles

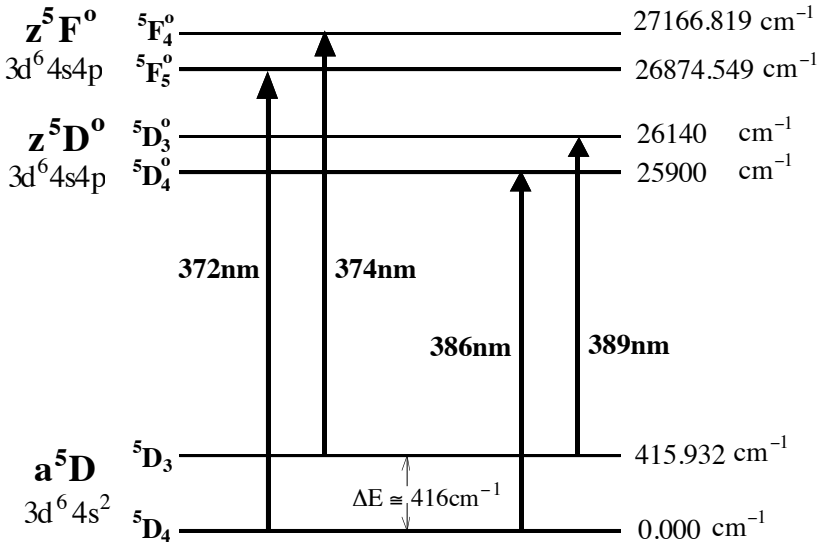

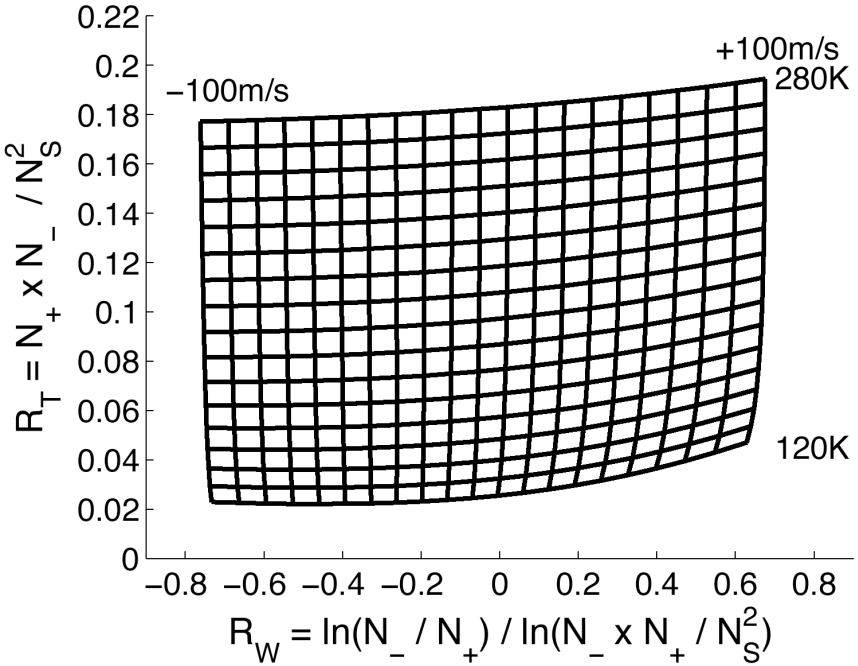

[Chu et al., ILRC, 2008]

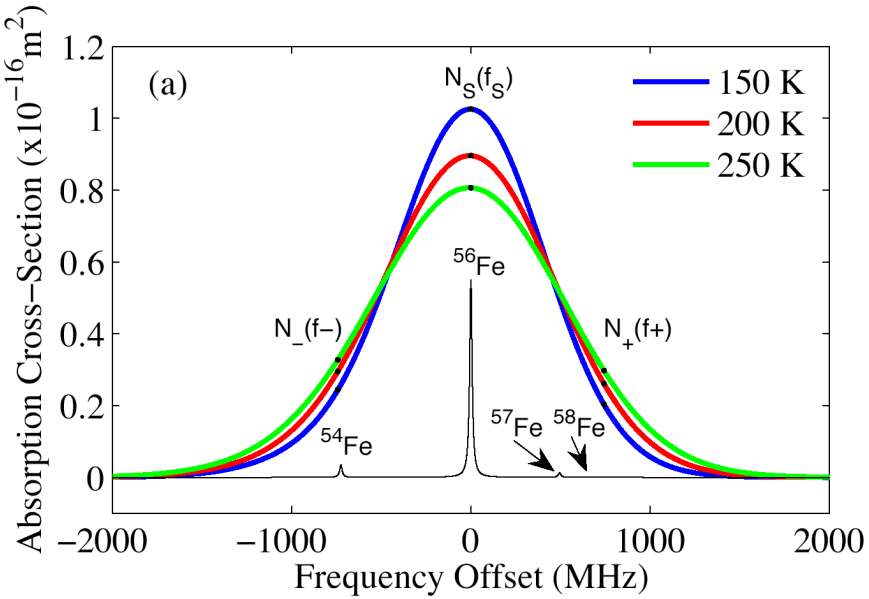

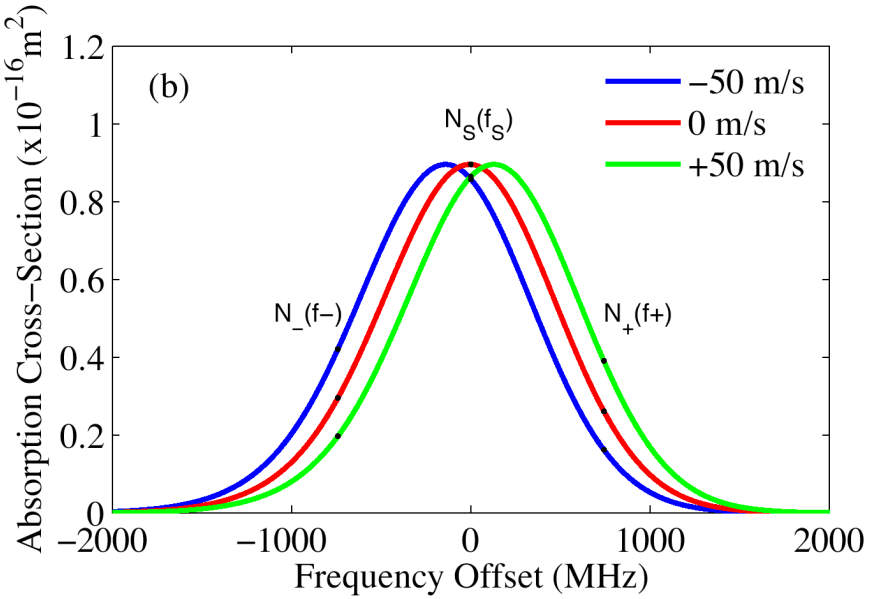

Fe (iron) 372-nm line

MRI Fe Doppler Lidar

[Chu et al., ILRC, 2010]

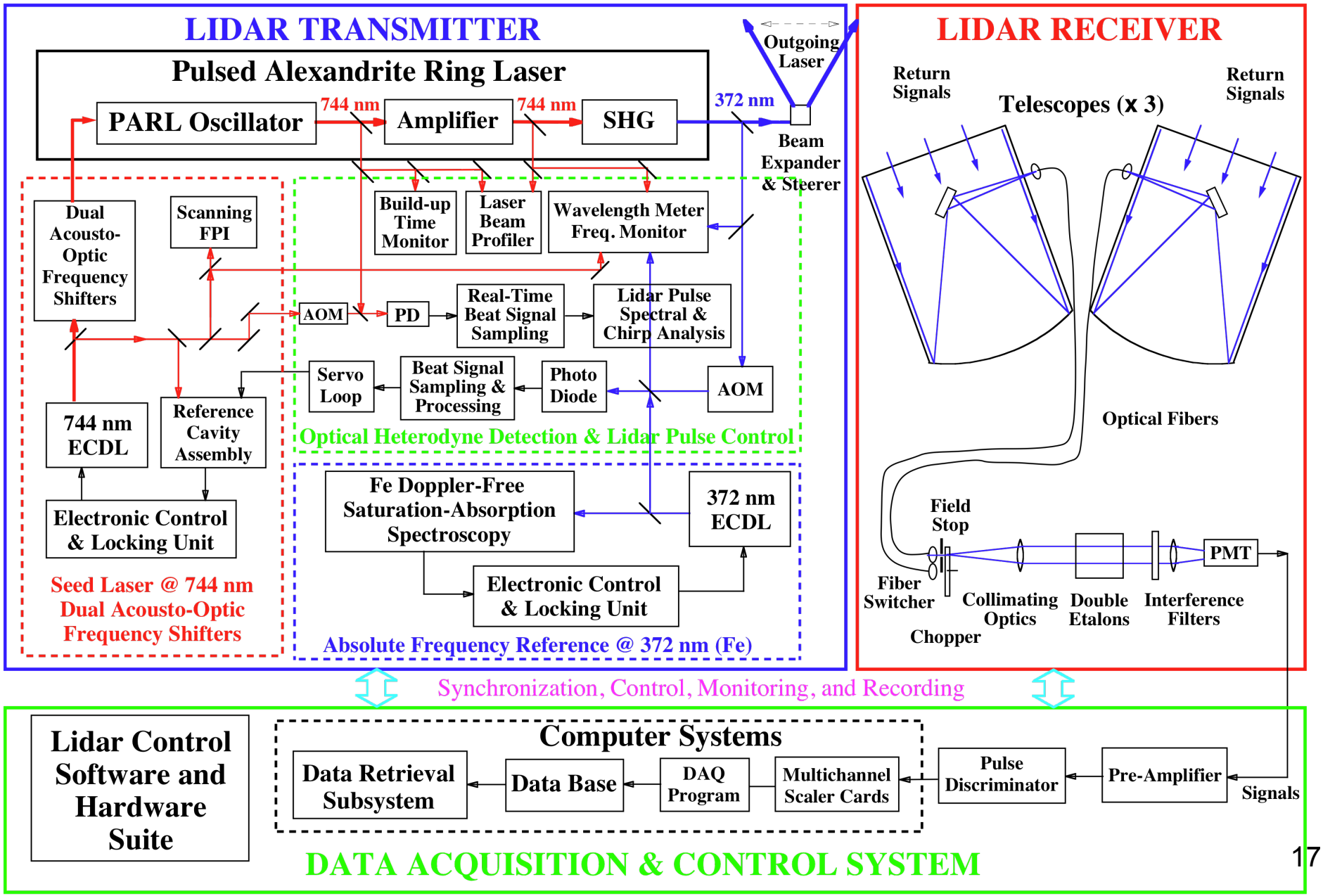

Optical Heterodyne Detection of Laser Pulse

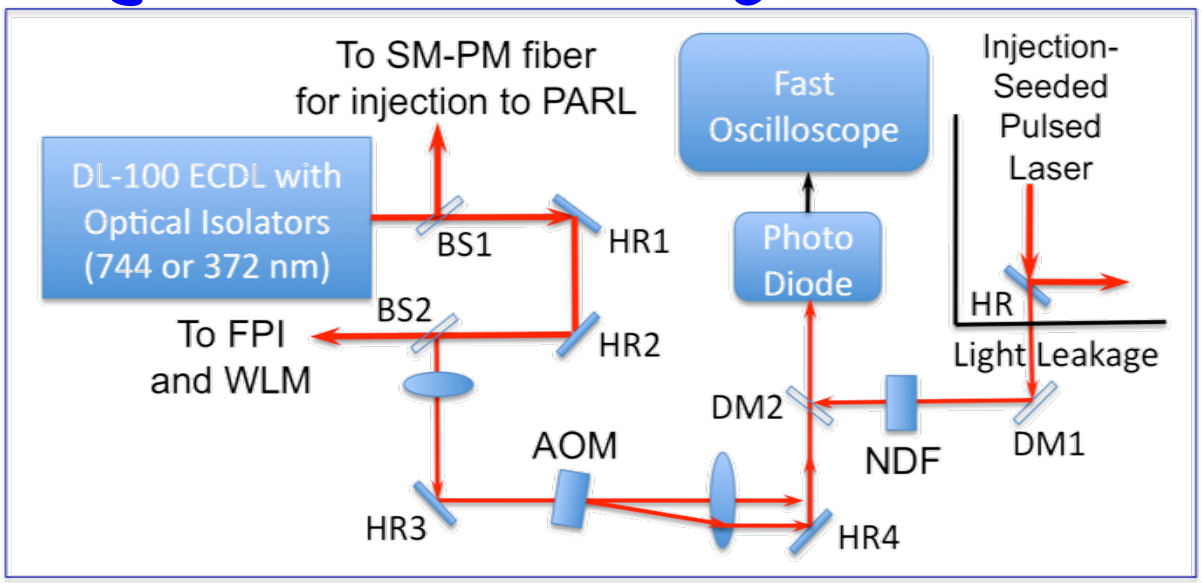

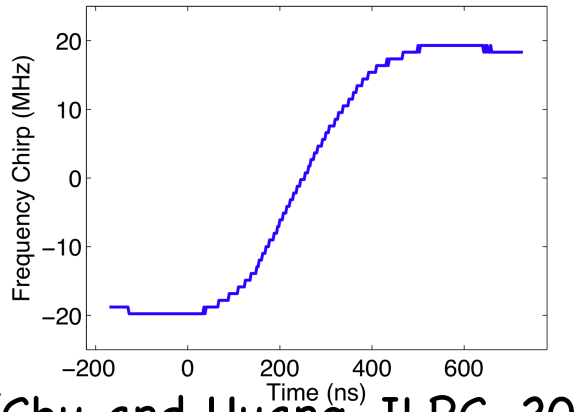

[Chu and Huang, ILRC, 2010]

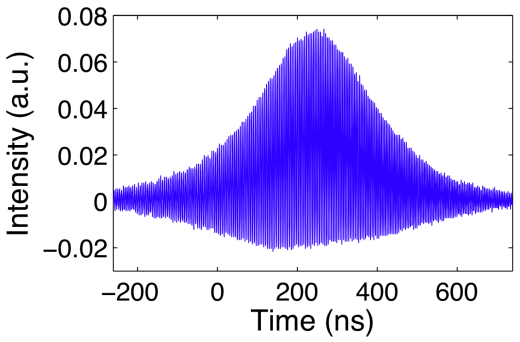

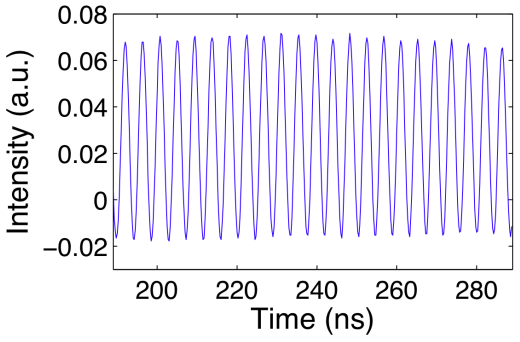

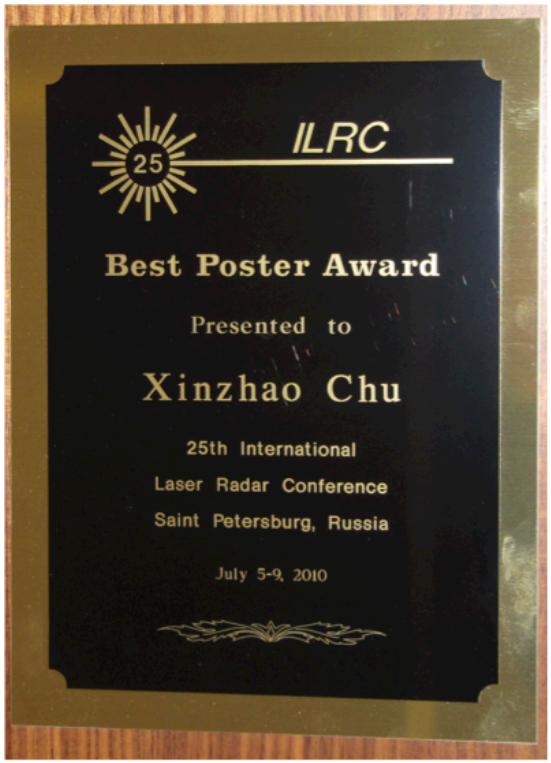

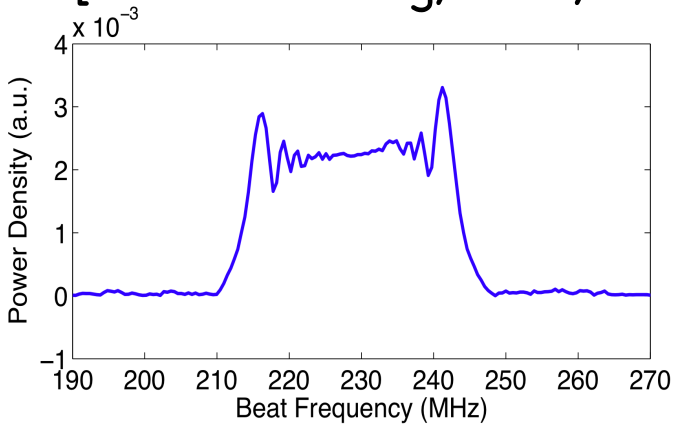

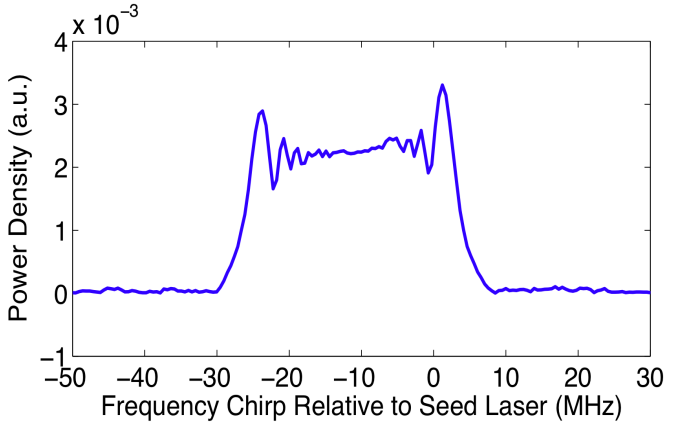

Mobile MRI Fe Doppler Lidar

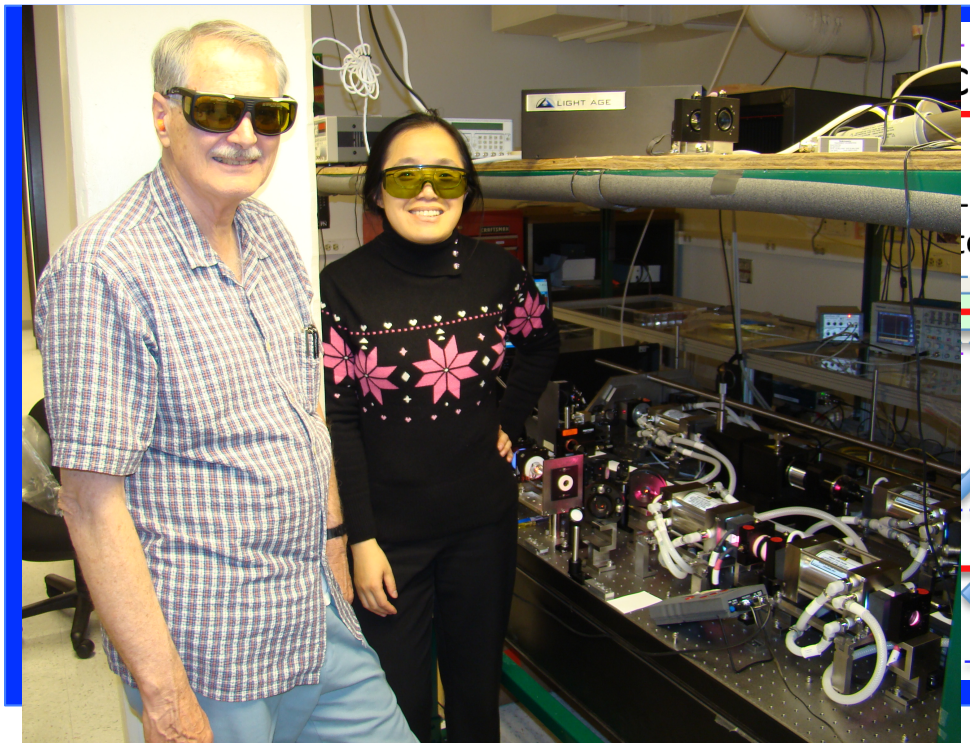

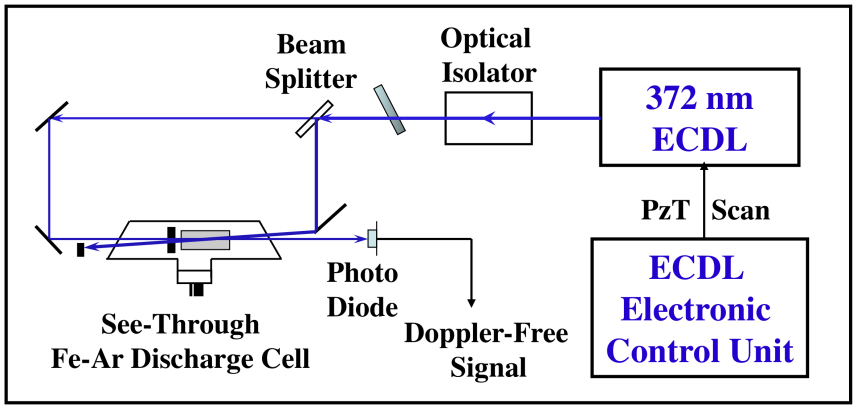

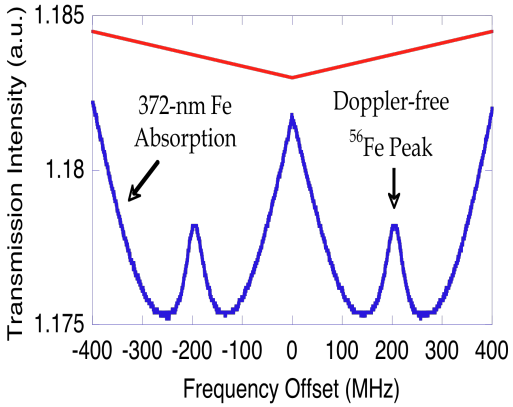

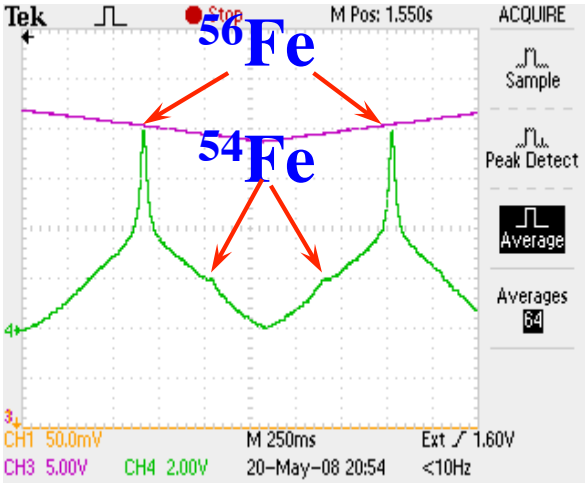

Fe Doppler-free spectroscopy at 372 nm and isotope identification obtained with the MRI Fe Doppler lidar.

Mobile MRI Fe Doppler Lidar At Table Mountain, Boulder

Pulsed Alexandrite Ring Laser (PARL) Based Narrowband 3-frequency Doppler Lidar for Wind, temperature and Fe density

Primary focus 81-cm telescope with fiber coupling

MRI Fe Doppler LIDAR – First Light

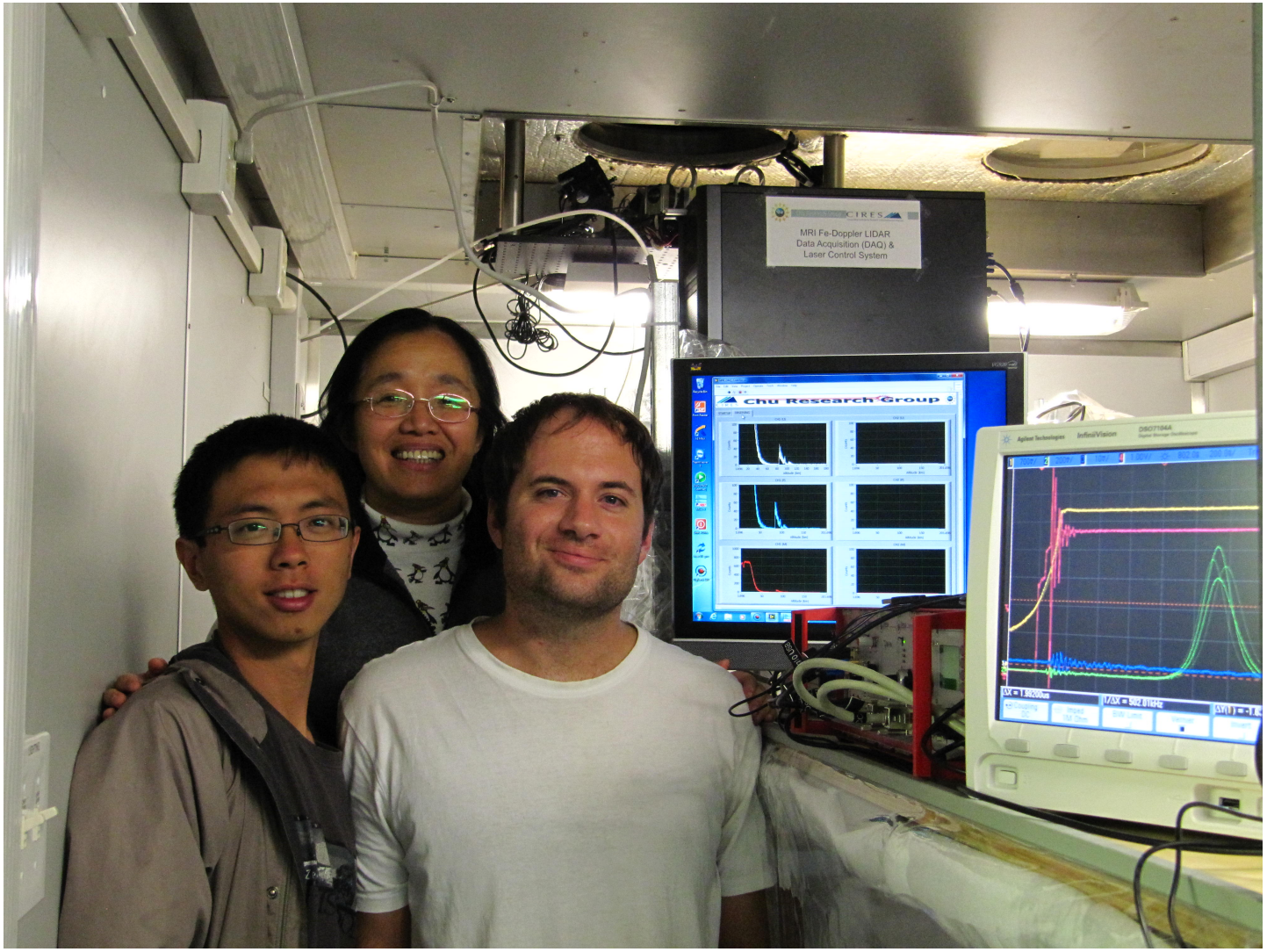

Containerized MRI lidar – hard to take photos
Come to Table Mountain to see it by your own eyes!

IAP Scanning Fe Doppler Lidar

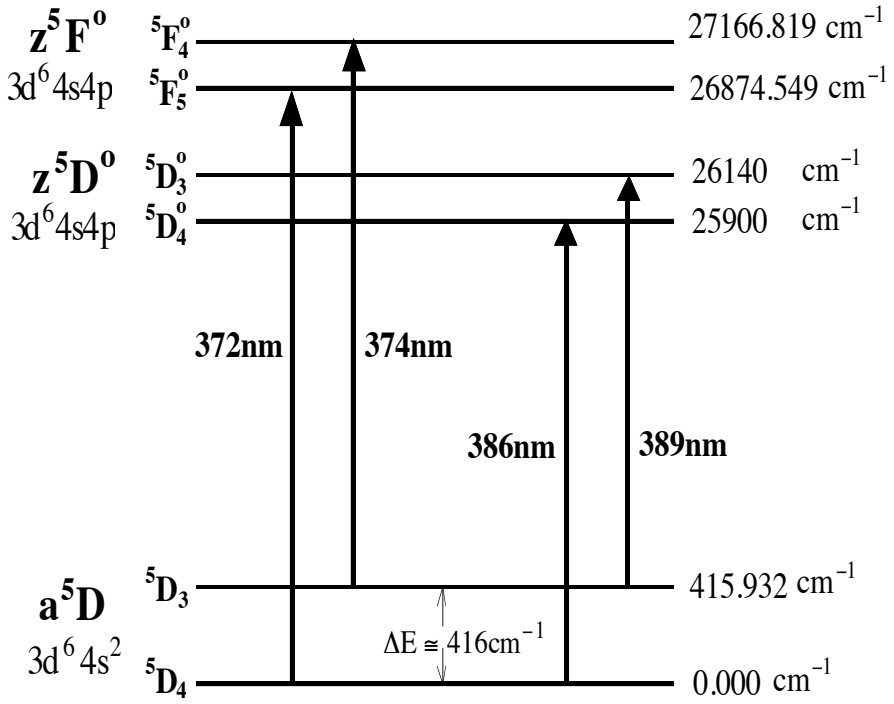

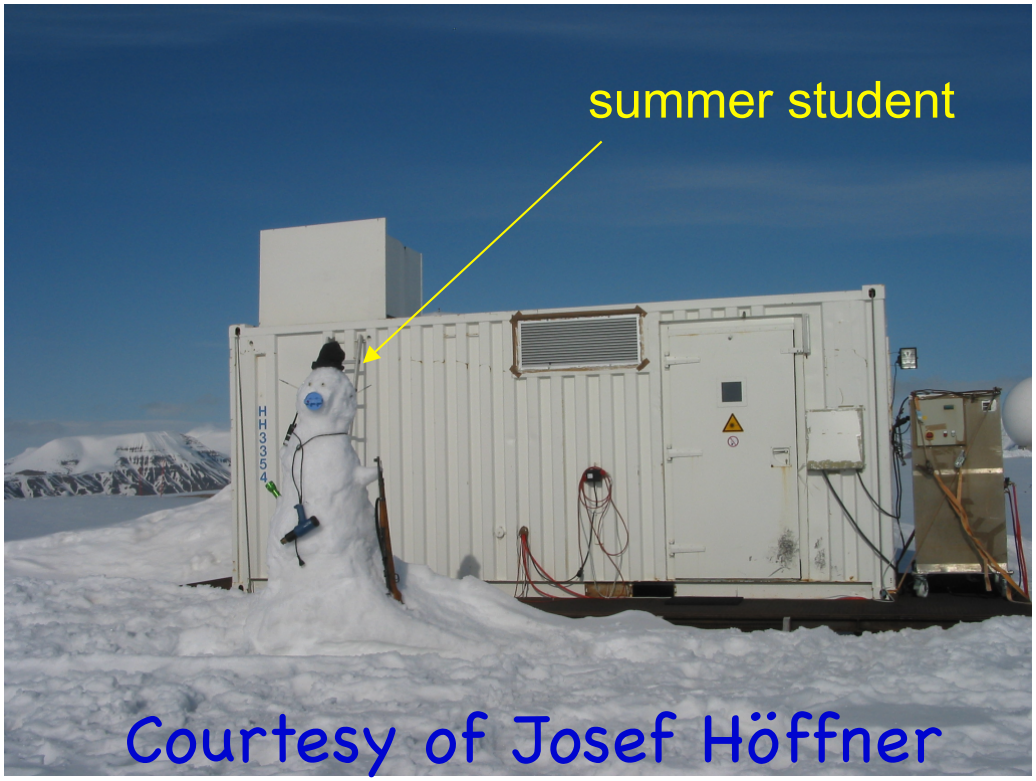

- IAP pulsed alexandrite ring laser was tuned from 770 nm to 772 nm, and then frequency doubled to probe the 386-nm Fe absorption line for temperature measurements with scanning technique developed for K Doppler lidar.
- Superior performance over K lidar due to Fe abundance, ..

Options for Na Doppler Lidar

- Conventional: Ring Dye Laser + PDA
- Hybrid: Solid-state cw 589nm source + PDA
  - -- CW Nd:YAG lasers SFG (1064 and 1319 -> 589 nm)
  - -- CW fiber lasers SFG (1583 and 938 -> 589 nm)
  - -- Raman shifted fiber laser SHG (1178->589 nm)
  - -- ECDL/DFB + Tapered Amplifier + SHG (1178->589 nm) Toptica
- Full solid-state pulsed 589nm laser
  - -- Flashlamp pumped Nd:YAG lasers SFG
  - -- Diode-laser pumped Nd:YAG laser SFG
  - -- Self-Raman Nd:YVO_4 pulsed laser: 1064->1178->589 nm
- Solid-state cw 589nm laser + pseudorandom modulation or cw 589nm laser + bistatic configuration

Solid-State Na Doppler Lidar

- Japanese Shinshu system by Kawahara et al.: Frequency mixing of two Nd:YAG lasers at 1064 and 1319 nm

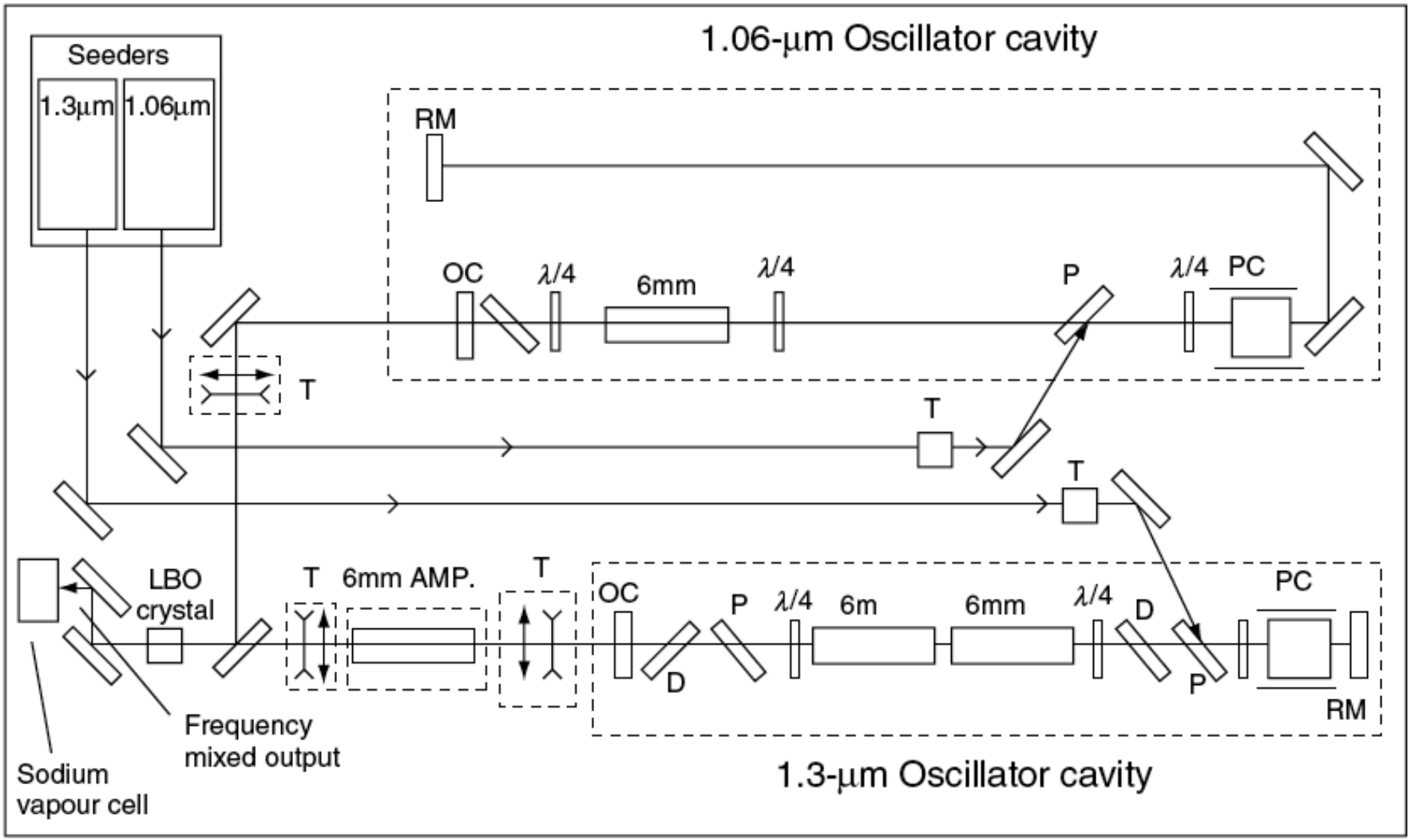

Solid-State Na Doppler Lidar Based on Diode-Laser-Pumped Nd:YAG Lasers

[Kawahara et al., ILRC, 2008]

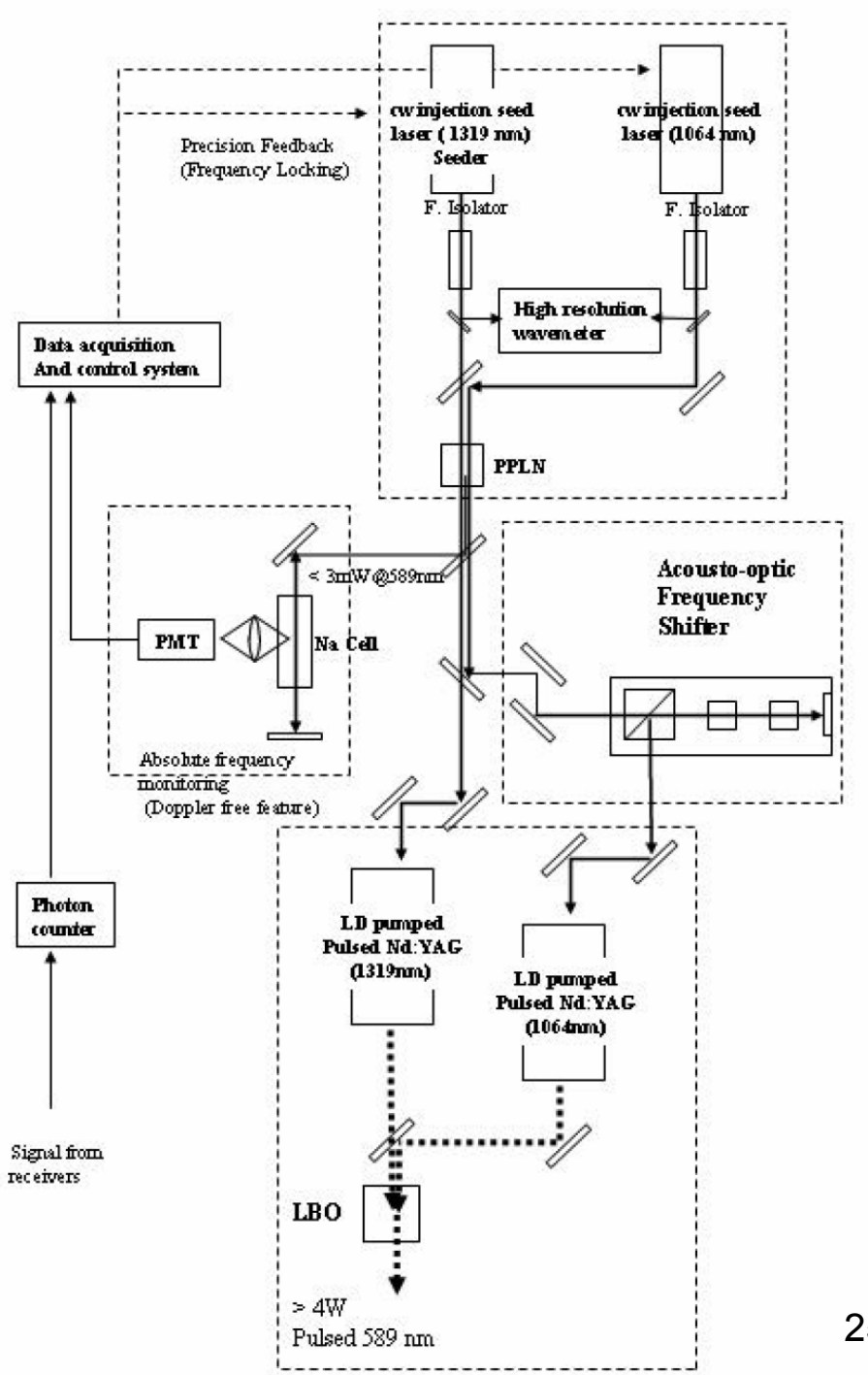

Summary (1)

- Currently state-of-the-art Na Doppler lidar is the dye-laser-based Na wind and temperature lidar - "ring dye laser + pulsed dye amplifier" configuration.
- One main feature is the narrowband Na lidar transmitter with precise frequency control and narrow laser linewidth: Na Doppler-free fluorescence spectroscopy for frequency calibration and locking, acousto-optic frequency modulator for generating two wing frequencies with high stability and fast switching, pulsed amplification with very low ASE.
- The lidar receiver (broadband) and DAQ subsystems have various styles and forms. They are also progressing rapidly.
- Na Doppler lidar can be realized with other laser configurations, e.g., solid-state Nd:YAG laser frequency mixing, or alexandrite laser Raman shift, etc.

Summary (2)

- There are several different atomic species originating from meteor ablation in the mesosphere and lower thermosphere (MLT) region. They all have the potentials to be tracers for resonance fluorescence Doppler lidars to measure the temperature and wind in MLT region.
- Na and K Doppler lidars are currently near mature status and are making great contributions to MLT science.
- Fe Doppler lidar has very high potential due to the high Fe abundance, advanced alexandrite laser technology, Fe Doppler-free spectroscopy, optical heterodyne detection technology, and bias-free measurement, etc.
- Solid-state Doppler lidars are demanded for science advancement, e.g., space exploration, although dye-laser-based Na Doppler lidar is still the golden standard for now. New Doppler lidar will surpass the classic Na lidar soon!